Available online at www.sciencedirect.com
SCIENCE DIRECT
Developmental Biology 292 (2006) 506–518
DEVELOPMENTAL BIOLOGY
www.elsevier.com/locate/ydbio

Genomes & Developmental Control

The *caudal*-related homeobox genes *cdx1a* and *cdx4* act redundantly to regulate *hox* gene expression and the formation of putative hematopoietic stem cells during zebrafish embryogenesis

Alan J. Davidson [1], Leonard I. Zon *

Division of Hematology/Oncology, Children's Hospital and Dana Farber Cancer Institute, Department of Pediatrics and Howard Hughes Medical Institute, Harvard Medical School, Karp Building 7, 1 Blackfan Circle, Boston, MA 02115, USA

Received for publication 7 September 2005; revised 21 November 2005; accepted 3 January 2006
Available online 7 February 2006

Abstract

The *hox* genes play a central role in organogenesis and are implicated in the formation of hematopoietic stem cells (HSCs). The *cdx* genes encode homeodomain transcription factors that act as master regulators of the *hox* genes. In zebrafish, mutations in *cdx4* cause a severe, but not complete, deficit in embryonic blood cells. Here, we report the expression and function of *cdx1a*, a zebrafish *Cdx1* paralogue. Using morpholino-mediated knockdown of *cdx1a* in a *cdx4* mutant background, we show that a deficiency in both *cdx* genes causes a severe perturbation of *hox* gene expression and a complete failure to specify blood. The hematopoietic defect in *cdx*-deficient embryos does not result from a general block in posterior mesoderm differentiation as endothelial cells and kidney progenitors are still formed in the doubly deficient embryos. In addition, *cdx*-deficient embryos display a significant reduction in *runx1a*$^{+}$ putative HSCs in the zebrafish equivalent to the aorta–gonad–mesonephros (AGM) region. Overexpressing *hoxa9a* in *cdx*-deficient embryos rescues embryonic erythropoiesis in the posterior mesoderm as well as the formation of HSCs in the AGM region. Taken together, these results suggest that the *cdx-hox* pathway plays an essential role in the formation of both embryonic erythroid cells and definitive HSCs during vertebrate embryogenesis.

Keywords: *Cdx*; Caudal homeobox; *Hox*; Zebrafish; Hematopoiesis; Hematopoietic stem cells

Introduction

The formation of hematopoietic stem cells (HSCs) during vertebrate development occurs in successive stages in anatomically distinct sites (reviewed by Galloway and Zon, 2003). In amniotes, the first wave (known as embryonic or primitive hematopoiesis) originates in the yolk sac blood islands and is characterized by the formation of erythroid and endothelial cells. The equivalent site in zebrafish is known as the intermediate cell mass (ICM) and forms in an intra-embryonic location along the trunk. In addition, macrophages and granulocytes arise from a rostral site near the head, called the rostral blood island (RBI; reviewed by Davidson and Zon, 2004). The ICM forms at the trunk midline by the convergence of bilateral stripes of hematopoietic and vascular precursors. The molecular pathways responsible for regulating hematopoiesis are highly conserved between teleosts and mammals, and zebrafish orthologues of many critical mammalian regulatory genes have been isolated (Davidson and Zon, 2004). One of the earliest molecular markers of blood precursors is the *stem cell leukaemia* (*scl*) gene, which encodes a basic helix–loop–helix transcription factor (Gering et al., 1998; Liao et al., 1998). During zebrafish embryogenesis, transcripts for *scl* are first found in the posterior lateral mesoderm (intermediate mesoderm) between the 2- and 3-somite stages. By the 5-somite stage, a subpopulation of *scl*$^{+}$ cells co-expresses the erythroid-specific zinc finger transcription factor *gata1*, consistent with these cells becoming committed to the erythroid lineage

* Corresponding author. Fax: +1 617 730 0222.
E-mail address: zon@enders.tch.harvard.edu (L.I. Zon).
[1] Current address: Center for Regenerative Medicine, Massachusetts General Hospital, Department of Medicine, Harvard Medical School, Boston, MA 02114, USA.

0012-1606/$ - see front matter © 2006 Elsevier Inc. All rights reserved.
doi:10.1016/j.ydbio.2006.01.003

(Detrich et al., 1995). The remaining *scl*-expressing cells go on to express the vascular marker *flk1/vegfr2* and most likely correspond to angioblasts (Liao et al., 1997; Sumoy et al., 1997; Davidson et al., 2003).

In mammals, definitive hematopoiesis begins with the generation of HSCs in the region of the aorta, gonad, and mesonephros (AGM). AGM-derived HSCs appear to bud-off from a hemogenic endothelium that comprises the ventral wall of the dorsal aorta (reviewed by Godin and Cumano, 2002). The *runx1* transcription factor gene is expressed in these endothelial cells and is essential for definitive HSC activity (Okuda et al., 1996; Wang et al., 1996). The expression pattern of zebrafish *runx1a* closely mirrors that of the mouse orthologue (North et al., 1999) and includes the ventral endothelium of the trunk dorsal aorta (Burns et al., 2002; Kalev-Zylinska et al., 2002). Although HSC transplantation methodologies have yet to be applied to these *runx1a*$^{+}$ cells, based on their anatomic location and gene expression profile, they likely represent either definitive HSCs or their hemogenic precursors. These *runx1a*$^{+}$ cells are believed to migrate to the kidney, the adult site of hematopoiesis in zebrafish, as well as supply lymphoid progenitors to the thymus (reviewed by Trede et al., 2001).

The establishment of anterior–posterior (AP) positional identities within the embryo is dependent upon the homeobox transcription factors encoded by the *Hox* genes (Krumlauf, 1994). Within the vertebrate genome, these genes are grouped together in clusters (*Hoxa*, *Hoxb*, *Hoxc*, and *Hoxd*) and are expressed in overlapping domains along the AP axis with their anterior expression limits correlating to their physical order within the cluster. Perturbations in the anterior expression boundaries of *Hox* genes result in changes in cell fate, and this has led to the '*Hox* code' hypothesis, in which specific combinations of *Hox* genes are believed to specify tissue identities along the AP axis (Krumlauf, 1994). *Hox* genes have also been shown to influence hematopoietic lineage decisions, promote HSC proliferation, and induce leukemia when ectopically expressed. For example, overexpression of *Hoxb4* has been implicated in the proliferation/self-renewal of HSCs (Sauvageau et al., 1995; Antonchuk et al., 2002) and is capable of inducing embryonic stem (ES) cell-derived hematopoietic progenitors to acquire properties characteristic of adult HSCs (Kyba et al., 2002). Loss of *Hoxa9* in mice causes defects in both the granulocytic and lymphocytic lineages, whereas enforced expression is leukemogenic (reviewed by Lawrence et al., 1996).

Homeobox genes lying outside of the *Hox* clusters have also been implicated in AP patterning. Among these genes is *caudal*, which forms part of the recently identified para*hox* cluster that is most likely an evolutionary sister to the *Hox* complex (Brooke et al., 1998). In metazoans, the expression of *caudal* orthologues is localized to the posterior of the embryo (Mlodzik et al., 1985; Macdonald and Struhl, 1986; Gamer and Wright, 1993; Meyer and Gruss, 1993; Marom et al., 1997; Pillemer et al., 1998) and loss-of-function studies support a developmental role for *caudal* in determining the identity of the most posterior tissues (Wu and Lengyel, 1998; Katsuyama et al., 1999; Moreno and Morata, 1999; Edgar et al., 2001). In vertebrates, three *caudal* paralogues have been identified (known as *Cdx1*, *Cdx2*, and *Cdx4* in mammals). Gene targeting studies in the mouse have identified a role for *Cdx1* and *Cdx2* in the AP patterning of the vertebral column and tail formation (Subramanian et al., 1995; Chawengsaksophak et al., 1997; van den Akker et al., 2002; Chawengsaksophak et al., 2004). The axial skeleton defects in *Cdx1* and *Cdx2* mutants can be traced back to shifts in the expression boundaries of several *Hox* genes in the paraxial mesoderm (Subramanian et al., 1995; van den Akker et al., 2002). These results have led to the proposal that Cdx homeoproteins may transduce AP positional information by directly regulating *Hox* genes. An analysis of murine *Hoxb8* regulatory elements and overexpression studies in frogs supports this notion (Pownall et al., 1996; Epstein et al., 1997; Charité et al., 1998; Isaacs et al., 1998; Pownall et al., 1998).

Further evidence that members of the *cdx* family act as master regulators of the *hox* genes has come from the recent analysis of the zebrafish *kugelig* mutant, which is defective in *cdx4* (Davidson et al., 2003). *kugelig* embryos (herein referred to as *cdx4*$^{-/-}$ mutants or embryos) have a shortened AP axis and a severe deficit in ICM blood precursors that is correlated with shifts in the expression boundaries of multiple *hox* genes. By overexpressing specific *hox* genes, such as *hoxa9a*, it is possible to rescue the hematopoietic defect in *cdx4*$^{-/-}$ mutants. Furthermore, overexpression of mouse *Cdx4* in embryoid bodies alters *hox* gene expression and induces multi-potential hematopoietic progenitors (Davidson et al., 2003). These findings established a critical role for the *cdx-hox* pathway in the formation of blood cells during vertebrate embryogenesis.

Given that members of the *cdx* family are known to be functionally redundant and the fact that *cdx4*$^{-/-}$ mutants are not completely bloodless, we sought to identify additional zebrafish *cdx* genes that may act together with *cdx4*. In this report, we have characterized the expression and function of *cdx1a*, another member of the zebrafish *cdx* gene family. Using morpholino-mediated knockdown, we demonstrate that a deficiency in both *cdx1a* and *cdx4* leads to a failure to specify both ICM precursors and presumptive AGM-derived HSCs. The absence of ICM blood cells in embryos doubly deficient for *cdx1a* and *cdx4* and the AGM defect in *cdx4*$^{-/-}$ mutants can be rescued by overexpressing *hoxa9a*. These results demonstrate that *cdx1a* and *cdx4*, acting together, are necessary for the formation of both embryonic erythroid cells and definitive HSCs and provide further evidence to support a critical role for the *cdx-hox* pathway in controlling blood cell fate.

Materials and methods

Isolation of cdx1a by reverse transcriptase-polymerase chain reaction

Total RNA was isolated from the 5-somite stage wild-type embryos using established procedures (Chomczynski and Sacchi, 1987). First strand cDNA was synthesized using Superscript II RT (Invitrogen), according to the manufacturer's instructions, and used in a PCR reaction with the following *cdx1a* primers: forward (5′-ATG CGA ATT CAA ATG TCC GTG AGC TAT CTG-3′) and reverse (5′-GCA TGT CGA CCC CAA CAC TGC GTG TCA TTA-3′),

restriction enzyme sites underlined. The amplified product was purified, digested with *Eco*R1 and *Sal*1 and subcloned into the *Eco*R1 and *Xho*1 sites of pCS2^{+}.

Radiation hybrid mapping of cdx1a

cdx1a was mapped onto the Goodfellow radiation hybrid (RH) panel by the Children's Hospital Genome Initiative group using forward (5′-AGA CAC CTG AAC CTC AGC CA-3′) and reverse (5′-TGA TCC ACA GAT GGC AGC AC-3′) primers.

Whole mount in situ hybridization

Whole mount in situ hybridizations were performed as described (Paffett-Lugassy and Zon, 2004) using digoxigenin- or fluorescein-labeled antisense riboprobes. Transcripts were detected with alkaline-phosphatase-conjugated antibodies using the substrates BCIP/NBT (purple) or BCIP/INT (red).

Blood cell measurement

Embryos were flatmounted in 90% glycerol/PBST under a glass coverslip and then photographed using a digital camera (Coolpix 995, Nikon) mounted on a Leica MZ6 dissecting microscope. The captured images were enhanced using Photoshop 6.0 software (Adobe), and stained blood cells were counted on-screen by manually marking each cell. Four embryos were counted for each genotype and the statistical analysis performed using a two-tailed unpaired Student's *t* test. Genomic DNA was extracted from each embryo and genotyped by PCR as described below.

Microinjection

Synthetic messenger RNA for *hoxa9a* and *hoxb7a* was transcribed and injected as described previously (Davidson et al., 2003). The *cdx1a* morpholinos (antisense: CAG CAG ATA GCT CAC GGA CAT TTT C; 4 bp mis-match: CAT CAG ATA TCT CAC GTA CAT TGT C; mis-matched bases underlined) were purchased from Gene Tools LLC and solubilized in 1× Danieau solution. Embryos were injected with 1 nl of morpholino at a concentration of 0.3 mg/ml. For all injection experiments, at least 50 embryos were injected and analyzed.

Genotyping embryos

Genomic DNA was isolated from fixed embryos as described (Zhang et al., 1998), except that the concentration of proteinase K (PCR grade; Roche) was increased to 3.5 μg/μl in a final volume of 30 μl. To identify *cdx4* heterozygotes, the following primers that span the *kgg* deletion and amplify a 1.2 kb product in *cdx4*$^{+/-}$ (and *cdx4*$^{-/-}$) embryos were used: forward 5′-ACC GTC CAG TCG TCA TCA AC-3′, reverse 5′-GAG GTG AAC GTG CTA CCG AC. To confirm *cdx4*$^{-/-}$ mutants, the following primers (designed to exons 3 and 4 which are missing in the mutants) were used: forward 5′-CAA AAC GAG AAC GAA GGA GA-3′, reverse 5′-TGG ATG ATC CAA GTT CGA GT-3′. These primers amplify a 498 bp product in wild-type embryos or heterozygotes but fail to amplify a product in *cdx4*$^{-/-}$ mutants.

Results

Isolation and expression of cdx1a

A cDNA for *cdx1a* was isolated from 5-somite stage embryos by RT-PCR using primers designed to sequence deposited in GenBank by Shimizu et al., 2005. The predicted open reading frame of *cdx1a* encodes a protein of 229 amino acids (Fig. 1A) that is most similar to the protein encoded by the *cdx1* orthologue of *Xenopus tropicalis* (*Cad2*; 54% amino acid identity). Radiation hybrid (RH) mapping localized *cdx1a* to a region of linkage group (LG) 14 that shares synteny with *CDX1*, *SLC35A4*, and *CD84* on human chromosome (Hsa) 5q31–33 (Fig. 1B).

Expression of *cdx1a* during embryonic development was examined by whole mount in situ hybridization and was found to be similar to that reported by Shimizu et al. (2005). Transcripts for *cdx1a* are first detected at early gastrula stages in ventral marginal cells. During gastrulation, expression of *cdx1a* is maintained in both epiblast and hypoblast cells near the involuting marginal zone but is excluded from cells at the dorsal midline (data not shown and Fig. 1C). At this stage, the *cdx1a* expression domain is more extensive on the ventral side of the embryo (extending further towards the animal pole) than on the dorsal side. During early somitogenesis, *cdx1a* transcripts are found in cells of the posterior unsegmented paraxial mesoderm and tailbud. In our previous study, we found that *cdx4* and *scl* show a transient overlap in expression patterns at the 3-somite stage (Davidson et al., 2003), suggesting that the *cdx* genes may act in a cell-autonomous fashion during early blood development. A similar expression analysis for *cdx1a* and *scl* failed to show significant co-expression at the 3-somite stage (Fig. 1C), except for a few *scl*$^{+}$ cells in the posteriormost portion of the ICM stripes (data not shown). As somitogenesis proceeds, the expression domain of *cdx1a* in the unsegmented paraxial mesoderm becomes progressively more restricted, until only weak expression is detected in the tailbud, caudal fin mesenchyme, and cells of the posterior neural tube at the 22-somite stage (Fig. 1C and data not shown). At 48 h post-fertilization (hpf), transcripts for *cdx1a* are found in presumptive endodermal cells of the intestinal bulb and trunk gut tube (Fig. 1C).

Morpholino-mediated knockdown of cdx1a

To examine the role of *cdx1a* during development, we utilized an antisense morpholino designed to the *cdx1a* mRNA translational start site. Knockdown of *cdx1a* in a wild-type background resulted in no overt morphological defects (data not shown). In mice, *Cdx1* has been implicated in the autoregulation of its expression (Prinos et al., 2001; Béland et al., 2004). To determine whether knockdown of *cdx1a* had an effect on the expression of *cdx1a*, we examined *cdx1a* transcripts in the morphants at the 10-somite stage by whole mount in situ hybridization. Contrary to the mouse studies, in which Cdx1 positively regulates its promoter, we found that the *cdx1a* expression was inappropriately maintained in the rostral paraxial mesoderm of *cdx1a* morphants, as well as embryos doubly deficient in *cdx1a* and *cdx4* (Fig. 1D). This finding indicates that morpholino-induced knockdown of Cdx1a protein levels leads to an upregulation of *cdx1a* gene expression, suggesting that Cdx1a negatively regulates its own transcription. The reason for the discrepancy between mouse and zebrafish is unknown but may be related to either the timing of when *cdx1* transcripts are examined or species differences in *cdx1* promoter regulation.

Studies in mice have shown that *Cdx1*$^{-/-}$;*Cdx2*$^{+/-}$ mutants display AP patterning perturbations that are more severe than

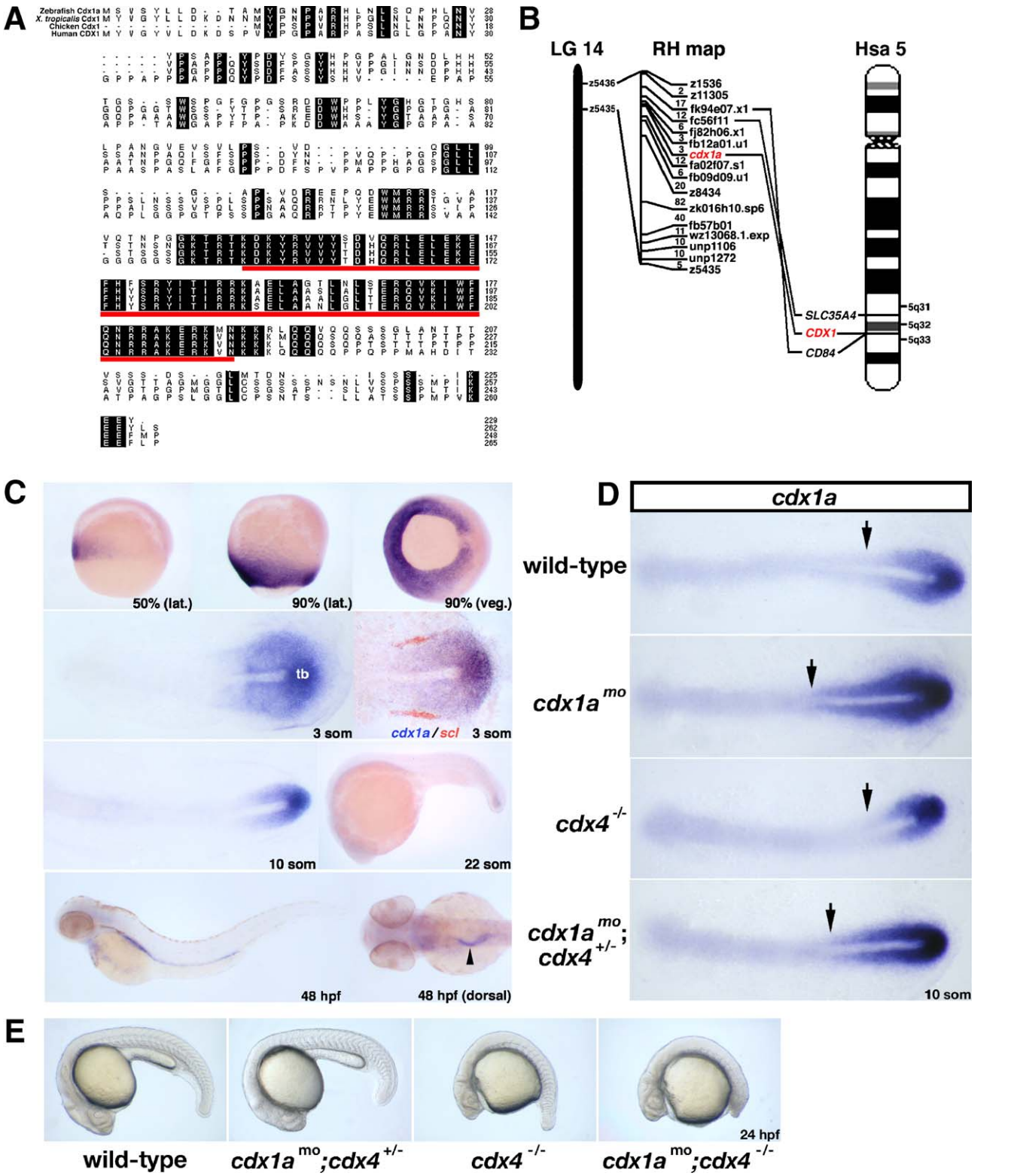

Fig. 1. Isolation, mapping, and functional characterization of *cdx1a*. (A) Predicted peptide alignment of Cdx1 proteins from zebrafish, *X. tropicalis*, chicken, and human. The sequence of the homeodomain is underlined in red. (B) Genetic and radiation hybrid map positions of *cdx1a* showing syntenic relationships with human chromosome (Hsa) 5q31–33. (C) Expression of *cdx1a* (purple) by whole mount in situ hybridization from 50% epiboly (early gastrula) to 48 h post-fertilization (hpf). Embryos in the top panels are oriented with their dorsal side to the right; all others are shown with anterior to the left. Embryos at the 3- and 10-somite stages have been flatmounted and are shown in dorsal views. Transcripts for *scl* at the 3-somite stage are stained red. Arrowhead indicates expression of *cdx1a* in the intestinal bulb at 48 hpf (shown in dorsal view). (D) Expression of *cdx1a* in a control-injected wild-type, *cdx1a* morphant, *cdx4* mutant, and an embryo doubly deficient for *cdx1a* and *cdx4*. Arrows indicate the anterior boundary of the *cdx1a* expression domain in the paraxial mesoderm. (E) Morpholino-mediated knockdown of *cdx1a*. Images of live embryos injected with *cdx1a* morpholinos ($cdx1a^{mo}$;$cdx4^{+/-}$ and $cdx1a^{mo}$;$cdx4^{-/-}$) or mis-match control morpholinos (wild type and $cdx4^{-/-}$) at 24 hpf. Embryos are shown in lateral views with anterior to the right. Abbreviations: lat., lateral view; veg., vegetal view; tb, tailbud.

either single mutation alone (*Cdx2*$^{-/-}$ mutants die at E3.5 due to trophectoderm defects), suggesting that the *Cdx* genes may act in a partially redundant fashion (van den Akker et al., 2002). To determine whether such an interaction exists between *cdx1a* and *cdx4*, we injected *cdx1a* morpholinos into embryos derived from *cdx4* heterozygous inter-crosses. Embryos either homozygous or heterozygous for the *cdx4* deletion were retrospectively genotyped by PCR. This analysis permitted *cdx4* gene dosage to be examined as *cdx1a* morphants carrying either one (*cdx1a*^{mo};*cdx4*$^{+/-}$) or two wild-type (*cdx1a*^{mo};*cdx4*$^{+/+}$) alleles of *cdx4* could be distinguished from doubly defective embryos (*cdx1a*^{mo};*cdx4*$^{-/-}$). Similar to results in a wild-type background, no overt morphological effects were seen when *cdx1a* was knocked down in *cdx4*$^{+/-}$ embryos (Fig. 1E and data not shown). However, doubly deficient (*cdx1a*^{mo};*cdx4*$^{-/-}$) embryos displayed more severe posterior truncations than control-injected *cdx4*$^{-/-}$ embryos (Fig. 1E). Concomitant with the shortened AP axis of *cdx1a*^{mo}/*cdx4*$^{-/-}$ embryos, only 8–12 somites formed in the doubly defective animals compared to *cdx4*$^{-/-}$ (28–30 somites) and wild-type embryos (30–32 somites). These results support a model in which *cdx1a* and *cdx4* act in a partially redundant fashion to regulate the formation of posterior tissues.

Expression of hox genes is perturbed in cdx-deficient embryos

We have previously shown that *cdx4*$^{-/-}$ mutants have altered expression patterns of several *hox* genes including *hoxb5a*, *hoxb7a*, and *hoxa9a* (Davidson et al., 2003). We therefore examined the effect of *cdx1a* and *cdx4* deficiency on the expression of these *hox* genes. In wild-type embryos at the 10-somite stage, the somitic expression of *hoxb5a* is restricted to somites two and three (Bruce et al., 2001) but is expanded caudally in *cdx4*$^{-/-}$ mutants to also include somites four and five (Davidson et al., 2003). In both *cdx1a*^{mo}/*cdx4*$^{+/+}$ and *cdx1a*^{mo}/*cdx*$^{+/-}$ embryos, the expression pattern of *hoxb5a* was similar to that of wild-type embryos (Fig. 2A and data not shown). In *cdx1a*^{mo}/*cdx4*$^{-/-}$ embryos, the expression domain of *hoxb5a* was significantly expanded caudally, with transcripts being detected in all of the somites posterior to somite one (Fig. 2A). Conversely, *hoxb7a* and *hoxa9a* showed reduced or absent expression domains in doubly defective embryos, respectively, compared to wild-type and *cdx4*$^{-/-}$ embryos (Fig. 2A and data not shown). Evidence for a *cdx4* gene dosage effect was seen for *hoxa9a*. While *cdx1*^{mo}/*cdx4*$^{+/+}$ animals showed wild-type levels of expression (data not shown), *cdx1a*^{mo}/*cdx4*$^{+/-}$ embryos displayed a shortened *hoxa9a* expression domain (Fig. 2A). Taken together, these findings are consistent with *cdx1a* and *cdx4* acting together to regulate *hox* gene expression along the AP axis and demonstrate that the transcriptional regulation of *hoxa9a* is particularly sensitive to *cdx* levels.

Embryonic blood, vascular, and pronephros development

To explore the role of *cdx1a* and *cdx4* during blood and vascular development, we examined the expression of *scl* in *cdx1a* morpholino-injected embryos. At the 5-somite stage, wild-type embryos express *scl* in juxtaposed populations of presumptive HSCs and angioblasts in both the RBI and the posterior ICM precursors (Davidson and Zon, 2004). Expression of *scl* in cells of the RBI was normal in embryos either singly or doubly deficient in *cdx1a* and *cdx4* (Fig. 2B and data not shown). Similarly, normal expression of *draculin* (*dra*) and *pu.1*, both of which encode transcription factors expressed by RBI myeloid progenitors (Herbomel et al., 1999; Bennett et al., 2001; Lieschke et al., 2002), was found at the 15-somite stage (Fig. 2B and data not shown). These results indicate that loss of *cdx1a* and/or *cdx4* has no effect on RBI hematopoiesis. In contrast, we found evidence that the development of ICM precursors is sensitive to *cdx4* gene dosage. Although knockdown of *cdx1a* alone (*cdx1a*^{mo};*cdx4*$^{+/+}$) has no effect on ICM development, *cdx1a*^{mo};*cdx4*$^{+/-}$ embryos display fewer *scl*$^{+}$ ICM precursors at the 5-somite stage, compared to wild-type controls (Fig. 2B). This defect is even more severe in doubly deficient embryos (*cdx1a*^{mo}/*cdx4*$^{-/-}$), with *scl* transcripts being restricted to a small population of presumptive angioblasts in the rostral ICM (Fig. 2B bracket). Despite this early reduction, a recovery in the number of *scl*-expressing cells is found in the posterior mesoderm of *cdx1*^{mo}/*cdx4*$^{-/-}$ embryos at the 15-somite stage (Fig. 2B). These *scl*$^{+}$ cells do not appear to be blood precursors as they fail to express the early blood-specific marker *dra* (Fig. 2B). Instead, the *scl*-expressing ICM precursors in *cdx1*^{mo}/*cdx4*$^{-/-}$ embryos are most likely angioblasts. Consistent with this, we found a similar spatiotemporal development of *flk1*$^{+}$ angioblasts in *cdx1*^{mo}/*cdx4*$^{-/-}$ embryos (Fig. 3A). Taken together, these finding suggest that the formation of ICM blood precursors, but not the adjacent angioblasts, is highly sensitive to *cdx* gene dosage, with the severity of the defect following the phenotypic order: *cdx1a*^{mo}; *cdx4*$^{-/-}$ > *cdx4*$^{-/-}$ > *cdx1a*^{mo};*cdx4*$^{+/-}$.

ICM angioblasts are formed in each of the genotypic classes, but their appearance is significantly delayed in doubly deficient embryos. Interestingly, the formation of the rostral-most ICM angioblasts (indicated by lines in Fig. 3A) is not delayed in *cdx1*^{mo}/*cdx4*$^{-/-}$ animals. Instead, a greater number of these *scl*$^{+}$ angioblasts are found in doubly deficient embryos (and to a lesser extent in *cdx4*$^{-/-}$ mutants) at the 15-somite stage, as compared to wild-type controls (Fig. 2B, bracket). This early expansion in rostral ICM angioblasts appears to lead to an increased number of *flk1*-expressing endothelial cells in the region of the Duct of Cuvier (common cardinal vein) in *cdx4*$^{-/-}$ and *cdx1a*^{mo};*cdx4*$^{-/-}$ embryos at 24 hpf (brackets in Fig. 3A).

In addition to blood and vascular precursors, the intermediate mesoderm also gives rise to progenitors of the embryonic kidney (pronephros). To examine the effect of *cdx* gene deficiency on kidney development, we examined the expression of the homeobox gene *pax2.1*, which is expressed by pronephric tubule and duct progenitors adjacent to ICM precursors, at the 10-somite stage. No effect on *pax2.1* expression was observed in *cdx1a*^{mo};*cdx4*$^{+/-}$ embryos, whereas *cdx4*$^{-/-}$ mutants displayed a slight caudal shift in the anterior expression border of *pax2.1* similar to that reported previously (Davidson et al., 2003 and Fig. 3B). In doubly deficient embryos, *pax2.1*$^{+}$ pronephric

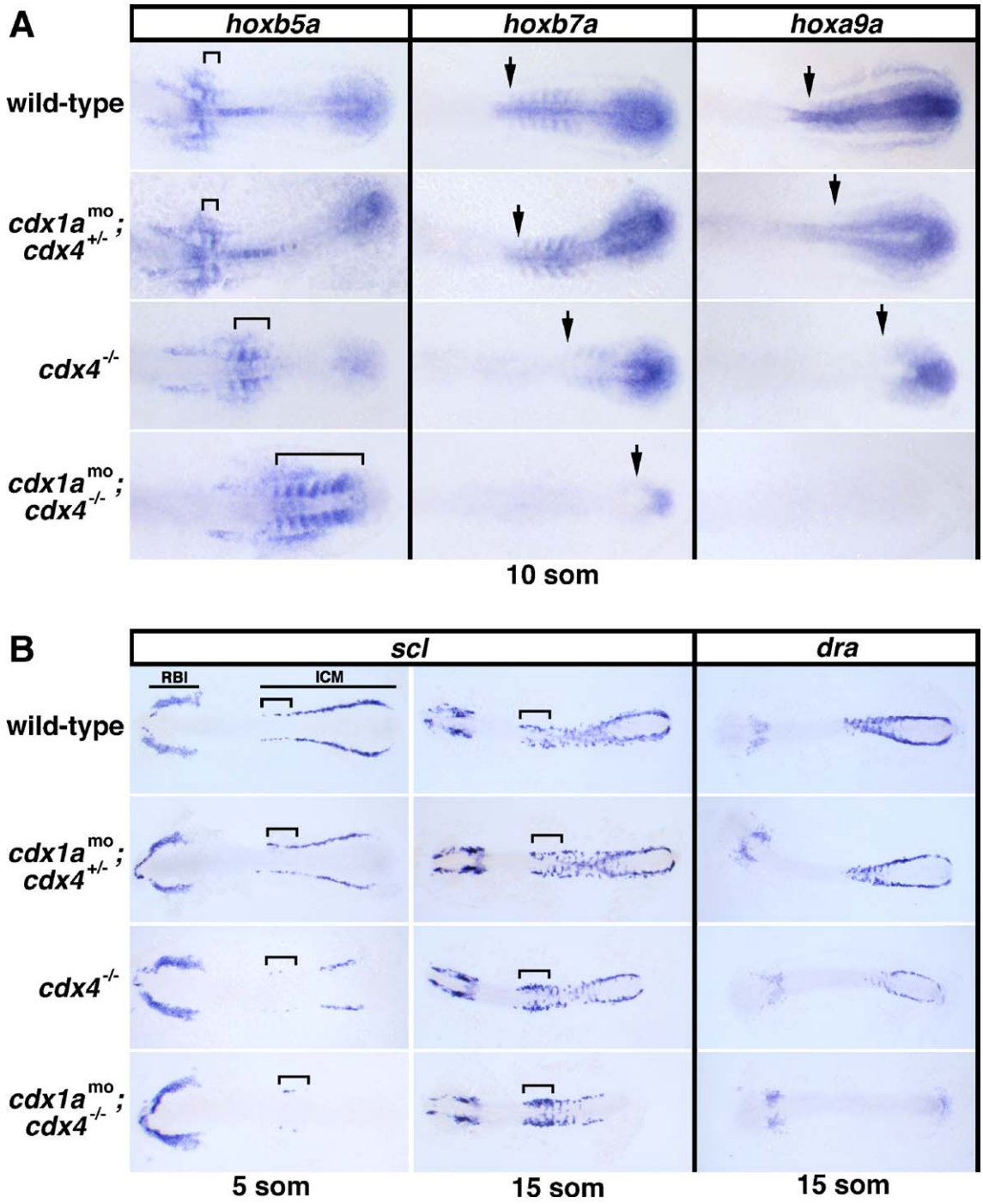

Fig. 2. Expression of *hox* genes, *scl*, and *dra* in *cdx*-deficient embryos. (A) Whole mount in situ hybridizations showing transcripts for *hoxb5a*, *hoxb7a*, and *hoxa9a* in *cdx*-deficient embryos and wild-type controls at the 10-somite stage. The extent of *hoxb5a* staining in the somites is indicated with a bracket. Arrows mark the anterior expression boundaries of *hoxb7a* and *hoxa9a* in the paraxial mesoderm. Dorsal views are shown, centered on the mid-trunk of flatmounted embryos, with anterior to the left. (B) Expression of *scl* and *dra* in *cdx*-deficient embryos and wild-type controls at the 5- and 15-somite stages. Note the *cdx* gene dosage effect on *scl*- and *dra*-expressing intermediate cell mass (ICM) precursor cells but not on rostral blood island (RBI)-derived cells. Presumptive angioblasts of the rostral ICM are indicated with a bracket and appear expanded in $cdx4^{-/-}$ and $cdx1a^{mo};cdx4^{-/-}$ embryos at the 15-somite stage. Flatmounted embryos are shown in dorsal views with anterior to the left.

progenitors were still found but were restricted to an even more posterior domain than that seen in $cdx4^{-/-}$ mutants. These results suggest that the spatial positioning but not the induction of pronephric progenitors is affected by a deficiency in *cdx* genes and further suggest that a general loss of posterior mesodermal fates is not responsible for the failure to specify ICM blood precursors in *cdx1a*/*cdx4*-deficient embryos.

To investigate the effect of *cdx1a* and *cdx4* gene dosage on erythroid development in more detail, we examined the expression of the erythroid-specific transcription factor gene

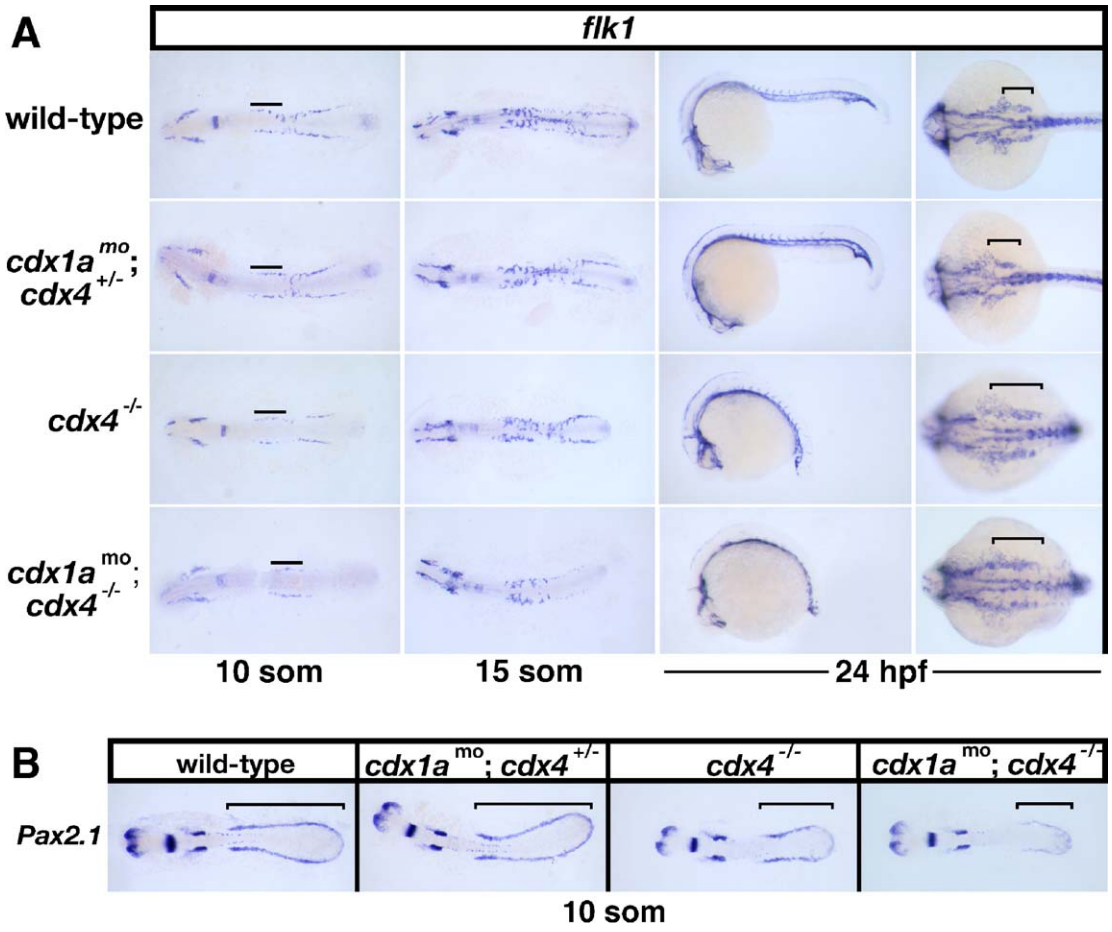

Fig. 3. Expression of *flk1* and *pax2.1* in *cdx*-deficient embryos. (A) Whole mount in situ hybridizations showing *flk1* transcripts (purple) in *cdx*-deficient embryos and wild-type controls at the 10- and 15-somite stages (flatmounted embryos shown in dorsal views with anterior to the left) and at 24 hpf (shown in lateral and dorsal views with anterior to the left). Lines mark the rostral angioblast populations. Brackets indicate the regions of *flk1*-expressing cells near the developing Duct of Cuvier. (B) Whole mount in situ hybridizations showing *pax2.1* expression (purple) in the pronephric progenitors (bracket) of wild-type and *cdx*-deficient embryos at the 10-somite stage. Flatmounted embryos are shown in dorsal views with anterior to the left.

gata1 between the 5-somite stage and 24 hpf (Fig. 4A). We also counted the number of $gata1^{+}$ cells in flatmounted embryos from each genotypic class at the 5-, 10-, and 18-somite stages (n = 4/class; Fig. 4B). As expected from our results with *scl* and *dra*, knockdown of *cdx1a* alone ($cdx1a^{mo}$/$cdx4^{+/+}$) had no effect on erythropoiesis, with morphants displaying a similar number of $gata1^{+}$ cells at the 5-, 10-, and 18-somite stages as wild-type embryos (Figs. 4A, B). Knockdown of *cdx1a* together with the loss of one wild-type *cdx4* allele ($cdx1a^{mo}$;$cdx4^{+/-}$) reduced the number of $gata1^{+}$ cells to approximately 50% of wild-type levels at the 5-somite and around 75% of wild-type levels by the 18-somite stage. This hematopoietic defect is more pronounced in $cdx4^{-/-}$ mutants, with the number of $gata1^{+}$ cells only reaching 40–50% of wild-type levels by the 18-somite stage. It is not until the 18-somite stage that *gata1* transcripts can be robustly detected in $cdx4^{-/-}$ mutants, suggesting that the onset of the *gata1* expression is also delayed in these animals. In $cdx1a^{mo}$; $cdx4^{-/-}$ embryos, an absence of both *dra* and *gata1* expression is consistent with a complete failure of the posterior mesoderm to specify ICM-derived blood precursors (Fig. 2B). In support of this, we were unable to detect *gata1* or embryonic *globin* transcripts as late as 36 hpf in doubly deficient embryos (data not shown). In summary, our analysis indicates that *cdx1a* and *cdx4* are essential for the formation of ICM blood precursors, but not angioblasts or pronephric progenitors, and that blood cell development is sensitive to *cdx* gene dosage.

Rescue of ICM hematopoiesis with hoxa9a

Erythroid differentiation, as assessed by the number of scl^{+} and $gata1^{+}$ cells, can be rescued in $cdx4^{-/-}$ mutants by overexpressing *hox* genes such as *hoxa9a* and *hoxb7a* (Davidson et al., 2003). These findings led us to suggest that a *cdx-hox* pathway is important for inducing embryonic erythroid cells during development. We therefore examined whether overexpressing *hoxa9a* and *hoxb7a* in $cdx1a^{mo}$;$cdx4^{-/-}$ embryos could restore erythropoiesis. Doubly deficient embryos injected with 3 pg of *hoxa9a* mRNA displayed a variable rescue of *gata1* expression at the 18-somite stage (61%; n = 11 of 18 mutants; Fig. 5A). In contrast, only a poor rescue was seen when $cdx1a^{mo}$;$cdx4^{-/-}$ embryos were injected with 3 pg of *hoxb7a* mRNA (12%; n = 3 of 25 mutants; Fig. 5A). These results indicate that *hoxa9a* is a more potent inducer of blood in

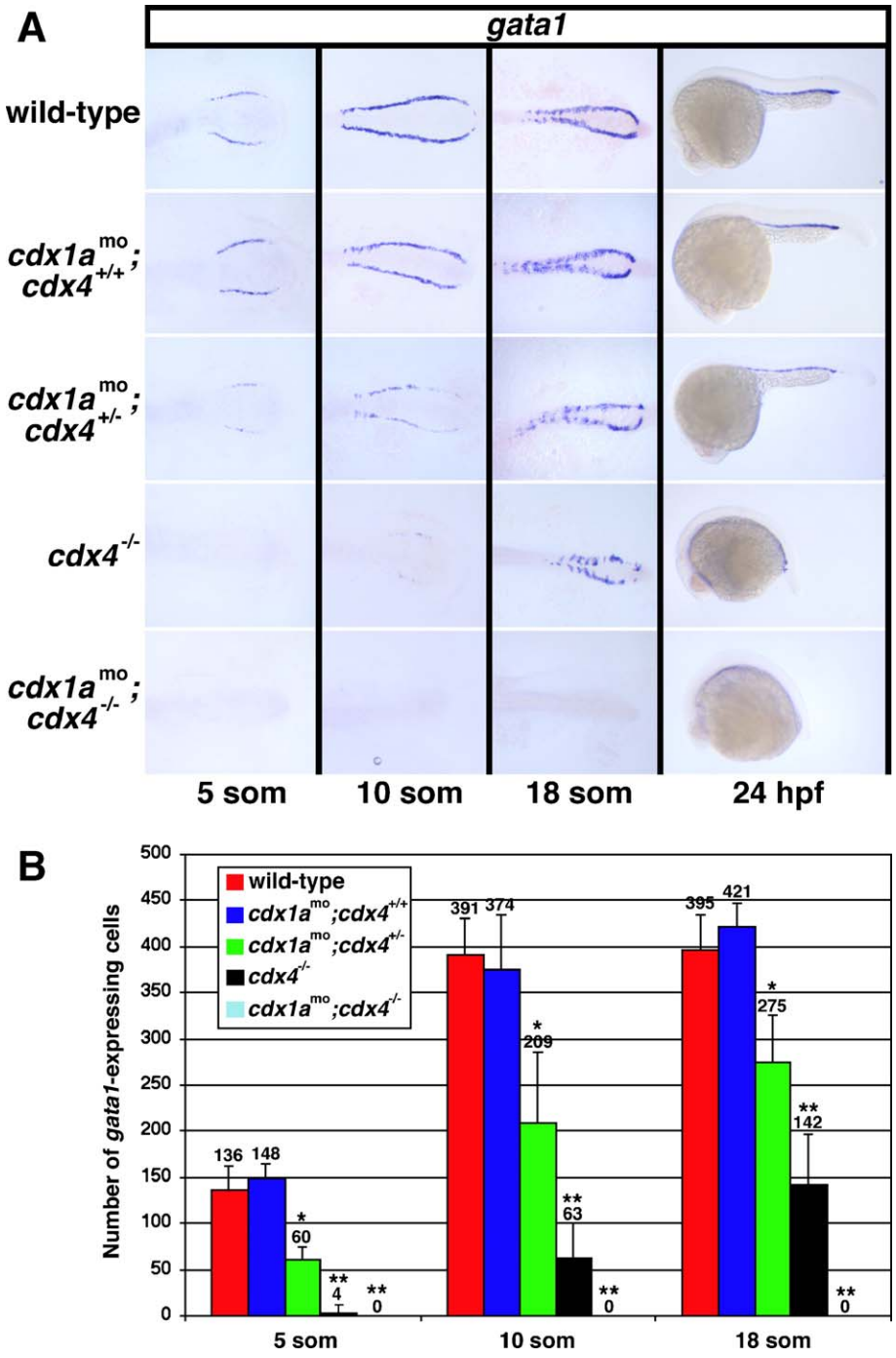

Fig. 4. Erythropoiesis in *cdx*-deficient embryos. (A) Whole mount in situ hybridizations showing *gata1* transcripts (purple) in *cdx*-deficient embryos and wild-type controls at the 5-, 10- and 18-somite stages (flatmounted embryos shown in dorsal views of the trunk with anterior to the left) and at 24 hpf (shown in lateral views with anterior to the left). (B) Bar graph showing the number of *gata1*-expressing cells in *cdx*-deficient and wild-type embryos at the 5-, 10-, and 18-somite stages. Values represent mean (indicated above each bar) ± SD ($n = 4$). *Significant difference $P < 0.01$; **Significant difference $P < 0.001$ compared to wild-type controls.

doubly deficient embryos than *hoxb7a*. At present, the reason for this difference is unclear. However, we did note a similar observation in our earlier study of *cdx4* mutants in which *hoxa9a* rescued 100% of $cdx4^{-/-}$ embryos, whereas *hoxb7a* was only able to rescue 65% of the mutants (Davidson et al., 2003). Overall, these findings support our hypothesis that *cdx1a* and *cdx4* act upstream of posterior *hox* genes such *hoxa9a* to specify ICM blood precursors.

Definitive hematopoiesis

A number of *Hox* genes are expressed by HSCs, and several have been implicated as regulators of self-renewal and lineage commitment (Owens and Hawley, 2002). Thus, we investigated whether *cdx1a* and *cdx4* were required for the generation of definitive HSCs. Knockdown of *cdx1a*, either alone ($cdx1a^{mo}$; $cdx4^{+/+}$) or in *cdx4* heterozygous embryos ($cdx1a^{mo}$;$cdx4^{+/-}$),

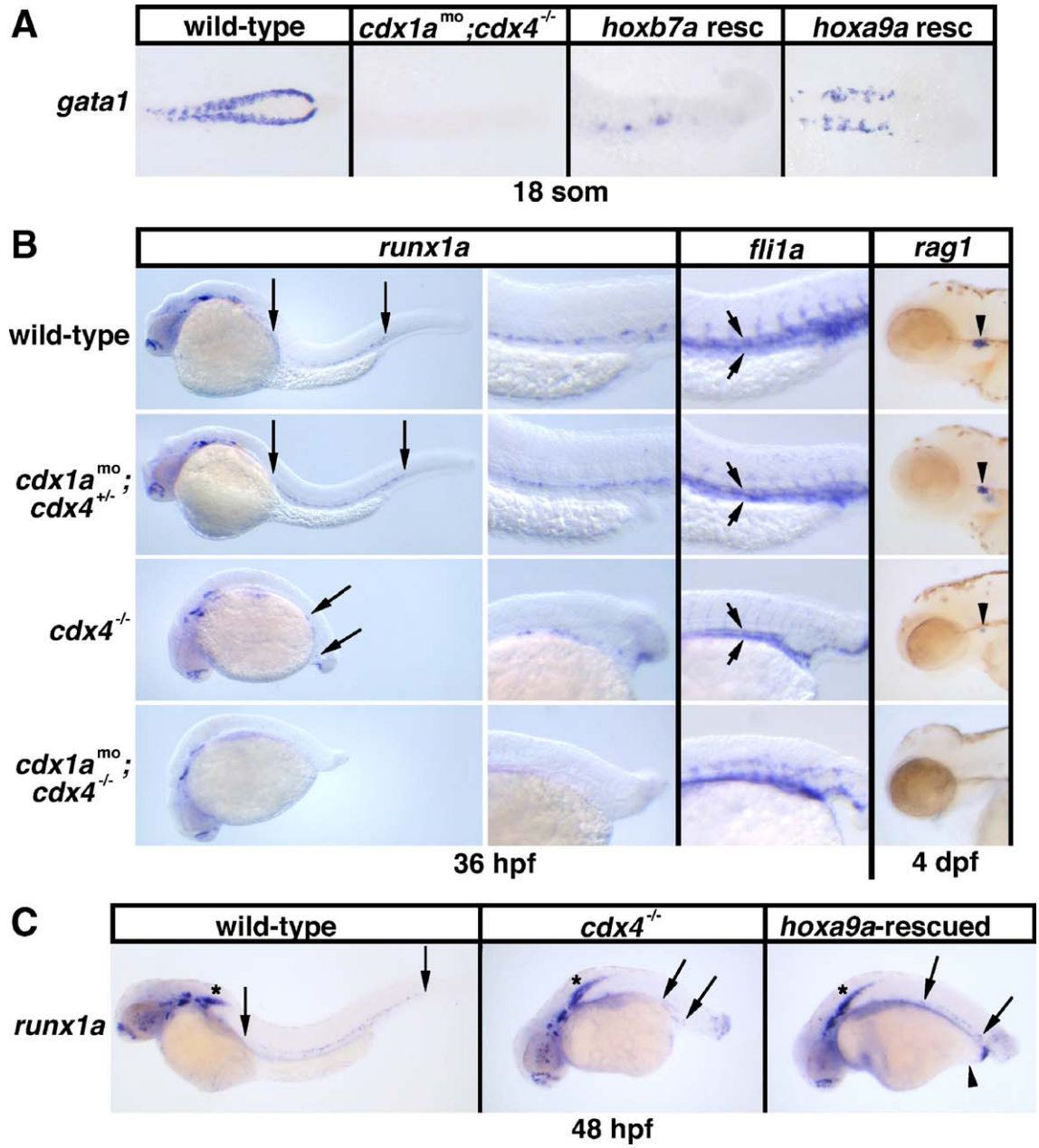

Fig. 5. Rescue of *gata1* and *runx1a* Expression in *cdx*-deficient Embryos. (A) Whole mount in situ hybridizations showing *gata1* transcripts (purple) in wild-type, doubly deficient (*cdx1a*^{mo};*cdx4*$^{-/-}$), *hoxb7a*-injected, and *hoxa9a*-injected doubly deficient embryos at the 18-somite stage (flatmounted embryos shown in dorsal views of the trunk with anterior to the left). (B) Expression of *runx1a*, *fli1a*, and *rag1* in *cdx*-deficient embryos (lateral views, anterior to the left). Arrows in the *runx1a*-stained embryos at 36 hpf indicate the extent of artery expression, and higher magnification views of the posterior trunk are shown alongside. A similar region in *fli1a*-stained embryos is shown with short arrows indicating the dorsal aorta and axial vein. Transcripts for *rag1* in the thymus of 4 dpf embryos are indicated by arrowheads. (C) Expression of *runx1a* in wild-type, *cdx4*$^{-/-}$ mutants, and *hoxa9a*-injected *cdx4*$^{-/-}$ embryos at 48 hpf. Arrows indicate the extent of *runx1a* staining in the dorsal aorta. Asterisks mark *runx1a*$^{+}$ cranial motorneurons in the hindbrain, and the arrowhead in the *hoxa9a*-rescued embryo indicates the short yolk tube extension.

had no effect on *runx1a* expression levels (Fig. 5B and data not shown). In *cdx4*$^{-/-}$ mutants, only the most posterior region of the trunk contains *runx1a*$^{+}$ cells, in contrast to wild-type embryos, where *runx1a* transcripts extend along the entire length of the dorsal aorta (Fig. 5B). Similar results were also found for *c-myb*, another gene expressed in presumptive HSCs (data not shown). In doubly deficient embryos, there was an absence of *runx1a* expression in the artery, despite relatively normal staining in other tissues (Fig. 5B). These results suggest that the formation of presumptive HSCs in the aorta is also affected by a deficiency in *cdx1a* and *cdx4*, although unlike the ICM, we found no evidence for a *cdx4* gene dosage effect.

Defects in the development of AGM-derived HSCs would be expected to have effects on the formation of definitive hematopoietic lineages such as lymphocytes. We therefore examined the expression of the *recombination activation gene-1*

(*rag1*), encoding a recombinase required for rearranging the T-cell receptor and immunoglobulin genes. Lymphoid cells in the bilateral thymi can be robustly detected by *rag1* expression at 4 days post-fertilization (reviewed by Trede et al., 2001). We found that *rag1* expression at 4 dpf was normal in *cdx1a* morphants, slightly reduced in *cdx4*$^{-/-}$ mutants, and absent in *cdx1a*^{mo};*cdx4*$^{-/-}$ doubly deficient embryos (Fig. 5B). Thus, a reduction in the number of *runx1a*$^{+}$ cells in the dorsal aorta at 36 hpf is associated with a concomitant decrease in the number of lymphocytes in the thymus at 4 dpf. These findings are consistent with *cdx1a* and *cdx4* being required for the formation of putative definitive HSCs.

Trunk angioblasts are formed in cdx-deficient embryos

It is conceivable that a reduction in the number of *runx1a*$^{+}$ cells in the dorsal aorta of *cdx4*$^{-/-}$ and *cdx1a*^{mo};*cdx4*$^{-/-}$ embryos may be caused by the defective formation of the artery itself. To investigate this, we stained the injected embryos at 36 hpf for *fli1a*, a gene encoding an ETS domain transcription factor that is expressed by the developing vasculature (Thompson et al., 1998; Brown et al., 2000). In *cdx4*$^{-/-}$ mutants, normal expression of *fli1a* is found in well-defined vessels of the dorsal aorta and axial vein along the trunk midline (arrows in Fig. 5B). Furthermore, blood cells can be seen circulating normally in *cdx4*$^{-/-}$ mutants, suggesting that the axial vessels are patent and functional. Thus, the *runx1a* deficiency in *cdx4*$^{-/-}$ mutants is not caused by a failure to form trunk vessels. Doubly deficient embryos display an increased number of *fli1a*$^{+}$ cells that are disorganized and scattered throughout the trunk (Fig. 5B). Furthermore, no obvious midline vessels are apparent in these embryos, suggesting that normal vasculogenesis is disrupted. Based on these observations, we cannot rule out that the more severe loss of *runx1a*-expressing cells in the dorsal aorta of *cdx1a*^{mo};*cdx4*$^{-/-}$ embryos is caused by defective vasculogenesis.

Rescue of runx1a expression with hoxa9a

We next investigated whether overexpressing *hoxa9a* in *cdx4*$^{-/-}$ mutants could rescue the defect in *runx1a* expression (rescues were not attempted in doubly deficient embryos given the severity of the vasculogenic defect). In 20% of *cdx4* mutants injected with 3 pg of *hoxa9a* mRNA ($n = 6/30$), the dorsal aorta displayed a greater number of *runx1a*$^{+}$ cells at 48 hpf, compared to uninjected *cdx4*$^{-/-}$ embryos (arrows in Fig. 5C). Although the rescued mutants displayed an overall morphology that was similar to uninjected *cdx4*$^{-/-}$ mutants, they did show signs of a partial rescue in posterior development with the formation of a short yolk tube extension (arrowhead in Fig. 5C). Nevertheless, the rescue of presumptive *runx1a*$^{+}$ HSCs was relatively specific as *cdx4*$^{-/-}$ mutants also display an expansion of *runx1a*$^{+}$ cranial motor neurons in the hindbrain (asterisk in Fig. 5C), but this defect was not rescued by *hoxa9a* overexpression. Thus, it appears that, although *hoxa9a* cannot fully substitute for the loss of *cdx4* function in all tissues, it is sufficient to partially rescue the development of presumptive HSCs from the dorsal aorta.

Discussion

In our previous study, we demonstrated that loss of *cdx4* results in an embryonic anemia that can be robustly rescued with *hoxb7a* and *hoxa9a* (Davidson et al., 2003). Over-expressing *cdx4* in zebrafish or mouse ES cells induces blood cell formation and alters *hox* expression levels. These results indicate that *cdx4*, acting upstream of the *hox* genes, plays a key role in specifying hematopoietic cell fate. However, *cdx4*$^{-/-}$ mutants are not bloodless nor completely devoid of posterior *hox* transcripts, raising the possibility that other members of the *cdx* family may co-operate with *cdx4*. In this report, we have characterized *cdx1a*, an additional member of the zebrafish *cdx* family, and shown that embryos deficient in *cdx1a* and *cdx4* lack all ICM-derived blood cells and display severe perturbations in *hox* expression domains. Furthermore, we have demonstrated that *cdx1a* and *cdx4* are also required for the formation of presumptive HSCs in the zebrafish AGM equivalent. Overexpression of *hoxa9a* in *cdx*-deficient embryos is sufficient to rescue the formation of both ICM and presumptive AGM HSCs, providing more evidence to support a central role for the *cdx-hox* pathway in hematopoietic development.

Redundancy between cdx1a and cdx4

The lack of an obvious morphological phenotype in wild-type embryos injected with *cdx1a* morpholinos suggests that *cdx4*, and potentially other members of the *cdx* gene family, can functionally compensate for the knockdown of *cdx1a*. In support of this, the expression pattern of *cdx1a* during gastrulation is similar to that of *cdx4*, and there is likely co-expression in the paraxial mesoderm during later stages. In the absence of a genetic null mutation in *cdx1a*, we cannot rule out that the *cdx1a* morphant phenotype is not hypomorphic, due to incomplete morpholino-mediated knockdown. In mice, *Cdx1* null mutants survive to adulthood, and, although they appear normal, they exhibit anterior transformations in the identity of the cervical and upper thoracic vertebrae (Subramanian et al., 1995). These alterations in the axial skeleton are associated with posterior shifts in the rostral expression boundaries of *Hox* genes such as *Hoxc5*, *Hoxa7*, *Hoxb8*, and *Hoxb9* (Subramanian et al., 1995; van den Akker et al., 2002). Although we have not examined the vertebrae of *cdx1a* morphants raised to adulthood, we did not observe alterations in the expression boundaries of *hoxb5a*, *hoxb7a*, or *hoxa9a* at earlier stages. Given these findings, it would appear that *cdx4*, and potentially other *cdx* genes, are able to fully compensate for the morpholino-mediated deficiency of *cdx1a*. On the other hand, loss of *cdx4* causes a relatively severe axial phenotype that is accentuated by the knockdown of *cdx1a*. These results suggest that *cdx1a* and *cdx4* function in a partially redundant fashion during the patterning and formation of the embryonic axis.

ICM hematopoiesis is sensitive to cdx gene dosage

Studies in mouse have demonstrated that loss of *Cdx1* and/or *Cdx2* causes gene-dosage-dependent homeotic vertebral transformations. *Cdx1* null mutants have a phenotype similar to double heterozygotes ($Cdx1^{+/-}$;$Cdx2^{+/-}$), whereas $Cdx1^{-/-}$; $Cdx2^{+/-}$ offspring exhibit the most severe alterations in vertebrae patterning and posterior truncation. Similarly, we found evidence for *cdx* gene dosage effects on hematopoietic development. Embryos heterozygous for *cdx4* are indistinguishable from wild-type siblings, but, when injected with *cdx1a* morpholinos ($cdx1a^{mo}$;$cdx4^{+/-}$), these animals manifest a reduction in the number of scl^{+} blood precursors and $gata1^{+}$ erythroid cells compared to uninjected controls. The hematopoietic defect of $cdx1a^{mo}$;$cdx4^{+/-}$ embryos is not associated with a shortening of the AP axis, which, in $cdx4^{-/-}$ mutants, also contributes to their blood deficit. Indeed, in terms of overall morphology, $cdx1a^{mo}$;$cdx4^{+/-}$ embryos appear identical to wild-type embryos. This suggests that the effect of the *cdx-hox* pathway on blood cell formation and posterior truncation can be separated. Consistent with this, the *hoxa9a* rescue of blood development in $cdx4^{-/-}$ and $cdx1a^{mo}$;$cdx4^{-/-}$ embryos does not appreciably rescue the posterior truncation defect (this study and Davidson et al., 2003).

The lack of significant overlap in the *cdx1a* and *scl* expression domains suggests that the *cdx* genes act non-cell-autonomously for blood development. However, the *tbx16* transcription factor gene, which is defective in the bloodless mutant *spadetail* and has a similar expression pattern to *cdx1a*, has both intrinsic and extrinsic effects on ICM blood formation (Rohde et al., 2004). Given this observation, we cannot rule out a cell-autonomous effect of *cdx1a* during ICM hematopoiesis. Despite this, the expression patterns of the posterior *hox* genes are predominantly expressed in the paraxial, but not intermediate mesoderm, and show little, if any, overlap with *scl* (A.J.D. and L.I.Z, unpublished results). If *cdx1a* and *cdx4* are required solely in the paraxial mesoderm during blood cell development, then downstream *hox* genes presumably control the production of secreted or cell-surface factor/s that in turn regulate HSC formation in the adjacent intermediate mesoderm. The finding that *hoxa9a* can robustly rescue erythropoiesis in both $cdx4^{-/-}$ and $cdx1a^{mo}$; $cdx4^{-/-}$ embryos and that *hoxa9a* expression is sensitive to *cdx* gene dosage makes the *hox* genes of the 9th paralogue group potential candidates for regulating these critical paraxial mesoderm factors.

The cdx-hox pathway is required for the formation of presumptive AGM-derived HSCs

At present, we have a poor understanding of the signaling pathways that operate upstream of *runx1* in the hemogenic endothelium. Our results, showing a severe reduction in the number of $runx1a^{+}$ endothelial cells in the artery of $cdx4^{-/-}$ mutants, suggest that the *cdx-hox* pathway plays an important role in the formation of AGM-derived HSCs. The few $runx1a^{+}$ cells that form in the mutants are localized near the most posterior portion of the artery, despite the aorta appearing equally well formed more anteriorly and functioning as a patent vessel. Thus, the *runx1a* defect appears to be specific to the hemogenic endothelium and is not caused by a general failure in vessel formation. We have been unable to find expression of *cdx1a*, *cdx4* or the *hox* genes *hoxb4a* and *hoxa9a* in the dorsal aorta at stages when putative $runx1a^{+}$ HSCs are arising (A.J.D. and L.I.Z., unpublished results). This raises the possibility that the *cdx-hox* pathway affects the generation of the $runx1a^{+}$ hemogenic endothelium by acting on angioblasts at earlier stages, prior to artery formation. Our observation that *cdx*-deficient embryos display an alteration in the number and patterning of anterior angioblasts supports an early role for the *cdx-hox* pathway in regulating vascular cell identity. The caudal shift in the anterior expression boundary of *runx1a* in the dorsal aorta of *cdx4* mutants mirrors the shifts seen with the *hox* expression domains, suggesting that the trunk angioblasts may have been homeotically transformed to a more anterior (and non-hemogenic) fate.

Similar to the rescue of ICM blood precursors, overexpression of *hoxa9a* in $cdx4^{-/-}$ mutants is sufficient to increase the extent of *runx1a* expression along the dorsal aorta at 48 hpf. However, rather than inducing *runx1a* transcripts in more anterior portions of the artery, *hoxa9a* overexpression expanded the *runx1a* expression domain caudally. This rescue correlated with a slight increase in the length of the trunk and a partial restoration of the yolk tube extension. Thus, the *hoxa9a* rescue of $runx1a^{+}$ cells in $cdx4^{-/-}$ mutants may be the result of a general increase in the formation or survival of posterior trunk tissue. Alternatively, as mentioned above, it is possible that the expression of *hox* genes or their downstream targets in the vascular precursors of the hemogenic endothelium may be needed for HSC formation at later stages. A recent study has demonstrated the importance of the *Mixed-lineage leukemia* (*MLL*) gene, encoding a Trithorax-related transcriptional regulator of *Hox* genes, in the development of AGM-derived HSCs (Ernst et al., 2004a). The AGM region of $Mll^{-/-}$ embryos shows reduced *runx1* expression and is unable to reconstitute hematopoiesis when transplanted into conditioned recipients. The in vitro differentiation of $Mll^{-/-}$ ES cells into blood cells can be rescued by overexpressing *Cdx4* (Ernst et al., 2004b), suggesting that *Mll* and *Cdx4* regulate a common set of *Hox* genes that are critical for hematopoietic development. Indeed, many of the *Hox* genes that are deregulated in $Mll^{-/-}$ embryos or cells (reviewed by Ernst et al., 2002) are also affected in $cdx4^{-/-}$ embryos (Davidson et al., 2003).

The efficiency of the *hoxa9a* rescue of $runx1a^{+}$ presumptive HSCs (20%) is less than that reported for embryonic hematopoiesis (100%; Davidson et al., 2003). This difference may be related to a lower efficacy of *hoxa9a* to rescue AGM-HSCs versus ICM precursors or factors inherent to the target tissue (for example, the intermediate mesoderm is a less complex tissue than the dorsal aorta and therefore is less likely to be affected by the non-specific effects of ectopic gene expression).

Implications of the cdx-hox pathway and oncogenesis

Dissecting how the *cdx*, *hox*, and *mll* genes function together to regulate HSC formation and differentiation will be the focus of future studies as it will permit these genes to be assembled into a transcriptional hierarchy. In addition to their role in hematopoiesis, members of the *cdx*, *hox* and *mll* gene families have also been implicated in leukemogenesis. For example, *Cdx2*, which likely has a functional overlap with *Cdx1* and *Cdx4*, is found ectopically expressed in one form of human acute myeloid leukemia (AML) and induces AML when overexpressed in the mouse bone marrow (Chase et al., 1999; Rawat et al., 2004). Similarly, enforced expression of several *Hox* genes, including *Hoxa7*, *Hoxb8*, and *Hoxa9*, induces leukemia in mice (Owens and Hawley, 2002). For AML, as well as other cancers, there is evidence for the existence of rare cancer stem cell populations that are responsible for maintaining the growth of the tumor (reviewed by Warner et al., 2004). Thus, the study of genes that control HSC formation in the embryo will not only provide a better understanding of HSC biology but may also lead to new therapeutic strategies to target cancer stem cells.

Acknowledgments

We thank Rebecca Wingert and Jenna Galloway for critical reading of the manuscript and Paula Fraenkel for help with the statistical analysis. We also thank members of the zebrafish community for gifts of cDNAs. L.I.Z. is an investigator of the Howard Hughes Medical Institute and is supported by grants from the NIH. A.J.D is funded by the Charles H. Hood Foundation, Inc., Boston and the Harvard Stem Cell Institute.

References

Antonchuk, J., Sauvageau, G., Humphries, R.K., 2002. *HOXB4*-induced expansion of adult hematopoietic stem cells ex vivo. Cell 109, 39–45.

Béland, M., Pilon, N., Houle, M., Oh, K., Sylvestre, J.-R., Prinos, P., Lohnes, D., 2004. *Cdx1* autoregulation is governed by a novel *Cdx1*–LEF1 transcription complex. Mol. Cell. Biol. 24, 5028–5038.

Bennett, C.M., Kanki, J.P., Rhodes, J., Liu, T.X., Paw, B.H., Kieran, M.W., Langenau, D.M., Delahaye-Brown, A., Zon, L.I., Fleming, M.D., et al., 2001. Myelopoiesis in the zebrafish, *Danio rerio*. Blood 98, 643–651.

Brooke, N.M., Garcia-Fernandez, J., Holland, P.W., 1998. The ParaHox gene cluster is an evolutionary sister of the Hox gene cluster. Nature 392, 920–922.

Brown, L.A., Rodaway, A.R., Schilling, T.F., Jowett, T., Ingham, P.W., Patient, R.K., Sharrocks, A.D., 2000. Insights into early vasculogenesis revealed by expression of the ETS-domain transcription factor Fli-1 in wild-type and mutant zebrafish embryos. Mech. Dev. 90, 237–252.

Bruce, E.E., Oates, A.C., Prince, V.E., Ho, R.K., 2001. Additional hox clusters in the zebrafish: divergent expression patterns belie equivalent activities of duplicate *hoxB5* genes. Evol. Dev. 3, 127–144.

Burns, C.E., DeBlasio, T., Zhou, Y., Zhang, J., Zon, L., Nimer, S.D., 2002. Isolation and characterization of *runxa* and *runxb*, zebrafish members of the runt family of transcriptional regulators. Exp. Hematol. 30, 1381–1389.

Charité, J., de Graaff, W., Consten, D., Reijnen, M.J., Korving, J., Deschamps, J., 1998. Transducing positional information to the Hox genes: critical interaction of *cdx* gene products with position-sensitive regulatory elements. Development 125, 4349–4358.

Chase, A., Reiter, A., Burci, L., Cazzaniga, G., Biondi, A., Pickard, J., Roberts, I.A.G., Goldman, J.M., Cross, N.C.P., 1999. Fusion of ETV6 to the caudal-related homeobox gene CDX2 in acute myeloid leukemia with the t(12;13)(p13;q12). Blood 93, 1025–1031.

Chawengsaksophak, K., James, R., Hammond, V.E., Kontgen, F., Beck, F., 1997. Homeosis and intestinal tumours in *cdx2* mutant mice. Nature 386, 84–87.

Chawengsaksophak, K., de Graaff, W., Rossant, J., Deschamps, J., Beck, F., 2004. Cdx2 is essential for axial elongation in mouse development. Proc. Natl. Acad. Sci. U. S. A. 101, 7641–7645.

Chomczynski, P., Sacchi, N., 1987. Single step method of RNA isolation by acid guanidinium thiocyanate-phenol-chloroform extraction. Anal. Biochem. 162, 156–159.

Davidson, A.J., Zon, L.I., 2004. The 'definitive' (and 'primitive') guide to zebrafish hematopoiesis. Oncogene 23, 7233–7246.

Davidson, A.J., Ernst, P., Wang, Y., Dekens, M.P., Kingsley, P.D., Palis, J., Korsmeyer, S.J., Daley, G.Q., Zon, L.I., 2003. *cdx4* mutants fail to specify blood progenitors and can be rescued by multiple *hox* genes. Nature 425, 300–306.

Detrich III, H.W., Kieran, M.W., Chan, F.Y., Barone, L.M., Yee, K., Rundstadler, J.A., Pratt, S., Ransom, D., Zon, L.I., 1995. Intraembryonic hematopoietic cell migration during vertebrate development. Proc. Natl. Acad. Sci. U. S. A. 92, 10713–10717.

Edgar, L.G., Carr, S., Wang, H., Wood, W.B., 2001. Zygotic expression of the *caudal* homolog *pal*-1 is required for posterior patterning in *Caenorhabditis elegans* embryogenesis. Dev. Biol. 229, 71–88.

Epstein, M., Pillemer, G., Yelin, R., Yisraeli, J.K., Fainsod, A., 1997. Patterning of the embryo along the anterior–posterior axis: the role of the *caudal* genes. Development 124, 3805–3814.

Ernst, P., Wang, J., Korsmeyer, S.J., 2002. The role of *MLL* in hematopoiesis and leukemia. Curr. Opin. Hematol. 9, 282–287.

Ernst, P., Fisher, J.K., Avery, W., Wade, S., Foy, D., Korsmeyer, S.J., 2004a. Definitive hematopoiesis requires the mixed-lineage leukemia gene. Dev. Cell 6, 437–443.

Ernst, P., Mabon, M., Davidson, A.J., Zon, L.I., Korsmeyer, S.J., 2004b. An Mll-dependent Hox program drives hematopoietic progenitor expansion. Curr. Biol. 23, 2063–2069.

Galloway, J.L., Zon, L.I., 2003. Ontogeny of hematopoiesis: examining the emergence of hematopoietic cells in the vertebrate embryo. Curr. Top. Dev. Biol. 53, 139–158.

Gamer, L., Wright, C.V.E., 1993. Murine *Cdx-4* bears striking similarities to the *Drosophila caudal* gene in its homeodomain sequence and early expression. Mech. Dev. 43, 71–81.

Gering, M., Rodaway, A.R.F., Göttgens, B., Patient, R.K., Green, A.R., 1998. The *SCL* gene specifies haemangioblast development from early mesoderm. EMBO J. 17, 4029–4045.

Godin, I., Cumano, A., 2002. The hare and the tortoise: an embryonic haematopoietic race. Nat. Rev., Immunol. 2, 593–604.

Herbomel, P., Thisse, B., Thisse, C., 1999. Ontogeny and behaviour of early macrophages in the zebrafish embryo. Development 126, 3735–3745.

Isaacs, H.V., Pownall, M.E., Slack, J.M.W., 1998. Regulation of *Hox* gene expression and posterior development by the *Xenopus caudal* homologue *Xcad3*. EMBO J. 17, 3413–3427.

Kalev-Zylinska, M.L., Horsfield, J.A., Flores, M.V.C., Postlethwait, J.H., Vitas, M.R., Baas, A.M., Crosier, P.S., Crosier, K.E., 2002. Runx1 is required for zebrafish blood and vessel development and expression of a human RUNX1-CBF2T1 transgene advances a model for studies of leukemogenesis. Development 129, 2015–2030.

Katsuyama, Y., Sato, Y., Wada, S., Saiga, H., 1999. Ascidian tail formation requires *caudal function*. Dev. Biol. 213, 257–268.

Krumlauf, R., 1994. *Hox* genes in vertebrate development. Cell 78, 191–201.

Kyba, M., Perlingeiro, R.C., Daley, G.Q., 2002. *HOXB4* confers definitive lymphoid-myeloid engraftment potential on embryonic stem cell and yolk sac hematopoietic progenitors. Cell 109, 29–37.

Lawrence, H.J., Sauvageau, G., Humphries, R.K., Largman, C., 1996. The role of *HOX* homeobox genes in normal and leukemic hematopoiesis. Stem Cells 14, 281–291.

Liao, W., Bisgrove, B.W., Sawyer, H., Hug, B., Bell, B., Peters, K., Grunwald,

D.J., Stainier, D.Y., 1997. The zebrafish gene *cloche* acts upstream of a *flk-1* homologue to regulate endothelial cell differentiation. Development 124, 381–389.

Liao, E.C., Paw, B.H., Oates, A.C., Pratt, S.J., Postlethwait, J.H., Zon, L.I., 1998. SCL/Tal-1 transcription factor acts downstream of cloche to specify hematopoietic and vascular progenitors in zebrafish. Genes Dev. 12, 621–626.

Lieschke, G.J., Oates, A.C., Paw, B.H., Thompson, M.A., Hall, N.E., Ward, A. C., Ho, R.K., Zon, L.I., Layton, J.E., 2002. Zebrafish SPI-1 (PU.1) marks a site of myeloid development independent of primitive erythropoiesis: implications for axial patterning. Dev. Biol. 246, 274–295.

Macdonald, P.M., Struhl, G., 1986. A molecular gradient in early *Drosophila* embryos and its role in specifying the body pattern. Nature 324, 537–545.

Marom, K., Shapira, E., Fainsod, A., 1997. The chicken *caudal* genes establish an anterior–posterior gradient by partially overlapping temporal and spatial patterns of expression. Mech. Dev. 64, 41–52.

Meyer, B.I., Gruss, P., 1993. Mouse *Cdx-1* expression during gastrulation. Development 117, 191–203.

Mlodzik, M., Fjose, A., Gehring, W.J., 1985. Isolation of *caudal*, a *Drosophila* homeo box-containing gene with maternal expression whose transcripts form a concentration gradient at the pre-blastoderm stage. EMBO J. 4, 2961–2969.

Moreno, E., Morata, G., 1999. The *Hox* gene *caudal* specifies the most posterior *Drosophila* segment and acts in combination with the Hedgehog pathway. Nature 400, 873–877.

North, T., Gu, T.L., Stacy, T., Wang, Q., Howard, L., Binder, M., Marin-Padilla, M., Speck, N.A., 1999. *Cbfa2* is required for the formation of intra-aotic hematopoietic clusters. Development 126, 2563–2575.

Okuda, T., van Deursen, J., Hiebert, S.W., Grosveld, G., Downing, J.R., 1996. *AML1*, the target of multiple chromosomal translocations in human leukemia, is essential for normal fetal liver hematopoiesis. Cell 84, 321–330.

Owens, B.M., Hawley, R.G., 2002. *HOX* and Non-*HOX* homeobox genes in leukemic hematopoiesis. Stem Cells 20, 364–379.

Paffett-Lugassy, N.N., Zon, L.I., 2004. Analysis of hematopoietic development in the zebrafish. Methods Mol. Med. 105, 171–179.

Pillemer, G., Epstein, M., Blumberg, B., Yisraeli, J.K., De Robertis, E.M., Steinbeisser, H., Fainsod, A., 1998. Nested expression and sequential downregulation of the *Xenopus caudal* genes along the anterior–posterior axis. Mech. Dev. 71, 193–196.

Pownall, M.E., Tucker, A.S., Slack, J.M.W., Isaacs, H.V., 1996. *eFGF*, *Xcad3* and *Hox* genes form a molecular pathway that establishes the anteroposterior axis in *Xenopus*. Development 122, 3881–3892.

Pownall, M.E., Isaacs, H.V., Slack, J.M.W., 1998. Two phases of *Hox* gene regulation during early *Xenopus* development. Curr. Biol. 8, 673–676.

Prinos, P., Joseph, S., Oh, K., Meyer, B.I., Gruss, P., Lohnes, D., 2001. Multiple pathways governing *Cdx1* expression during murine development. Dev. Biol. 239, 257–269.

Rawat, V.P., Cusan, M., Deshpande, A., Hiddemann, W., Quintanilla-Martinez, L., Humphries, R.K., Bohlander, S.K., Feuring-Buske, M., Buske, C., 2004. Ectopic expression of the homeobox gene Cdx2 is the transforming event in a mouse model of t(12;13)(p13;q12) acute myeloid leukemia. Proc. Natl. Acad. Sci. U. S. A. 101, 817–822.

Rohde, L.A., Oates, A.C., Ho, R.K., 2004. A crucial interaction between embryonic red blood cell progenitors and paraxial mesoderm revealed in *spadetail* embryos. Dev. Cell 7, 251–262.

Sauvageau, G., Thorsteinsdottir, U., Eaves, C.J., Lawrence, H.J., Largman, C., Lansdorp, P.M., Humphries, R.K., 1995. Overexpression of *HOXB4* in hematopoietic cells causes the selective expansion of more primitive populations in vitro and in vivo. Genes Dev. 9, 1753–1765.

Shimizu, T., Bae, Y.-K., Muraoka, O., Hibi, M., 2005. Interaction of Wnt and caudal-related genes in zebrafish posterior body formation. Dev. Biol. 279, 125–141.

Subramanian, V., Meyer, B.I., Gruss, P., 1995. Disruption of the murine homeobox gene *cdx1* affects axial skeletal identities by altering the mesodermal expression domains of Hox genes. Cell 83, 641–653.

Sumoy, L., Keasey, J.B., Dittman, T.D., Kimelman, D., 1997. A role for notochord in axial vascular development revealed by analysis of phenotype and the expression of VEGR-2 in zebrafish flh and ntl mutant embryos. Mech. Dev. 63, 15–27.

Thompson, M.A., Ransom, D.G., Pratt, S.J., MacLennan, H., Kieran, M.W., Detrich, H.W., Vail, B., Huber, T.L., Paw, B., Brownlie, B., et al., 1998. The *cloche* and *spadetail* genes differentially affect hematopoiesis and vasculogenesis. Dev. Biol. 197, 248–269.

Trede, N.S., Zapata, A., Zon, L.I., 2001. Fishing for lymphoid genes. Trends Immunol. 22, 302–307.

van den Akker, E., Forlani, S., Chawengsaksophak, K., de Graaff, W., Beck, F., Meyer, B.I., Deschamps, J., 2002. *Cdx1* and *Cdx2* have overlapping functions in anteroposterior patterning and posterior axis elongation. Development 129, 2181–2193.

Wang, Q., Stacy, T., Binder, M., Marin-Padilla, M., Sharpe, A.H., Speck, N.A., 1996. Disruption of the *Cbfa2* gene causes necrosis and hemorrhaging in the central nervous system and blocks definitive hematopoiesis. Proc. Natl. Acad. Sci. U. S. A. 93, 3444–3449.

Warner, J.K., Wang, J.C., Hope, K.J., Jin, L., Dick, J.E., 2004. Concepts of human leukemic development. Oncogene 23, 7164–7177.

Wu, L., Lengyel, J.A., 1998. Role of *caudal* in hindgut specification and gastrulation suggests homology between *Drosophila* aminoproctodeal invagination and vertebrate blastopore. Development 125, 2433–2442.

Zhang, J., Talbot, W.S., Schier, A.F., 1998. Positional cloning identifies zebrafish one-eyed pinhead as a permissive EGF-related ligand required during gastrulation. Cell 92, 241–251.